Magnetic-Field Control of Quantum Critical Points of Valence Transition

Shinji Watanabe,[1] Atsushi Tsuruta,[2] Kazumasa Miyake,[2] and Jacques Flouquet[3]

[1]*Department of Applied Physics, University of Tokyo, Hongo 7-3-1, Bunkyo-ku, Tokyo, 113-8656, Japan*
[2]*Division of Materials Physics, Department of Materials Engineering Science, Graduate School of Engineering Science,*
Osaka University, Toyonaka, Osaka 560-8531, Japan
[3]*Département de la Recherche Fondamentale sur la Matière Condenseé, SPSMS, CEA Grenoble,*
17 rue des Martyrs, 38054 Grenoble Cedex 9, France

We study the mechanism of how critical end points of first-order valence transitions are controlled by a magnetic field. We show that the critical temperature is suppressed to be a quantum critical point (QCP) by a magnetic field, and unexpectedly, the QCP exhibits nonmonotonic field dependence in the ground-state phase diagram, giving rise to the emergence of metamagnetism even in the intermediate valence-crossover regime. The driving force of the field-induced QCP is clarified to be cooperative phenomena of the Zeeman and Kondo effects, which create a distinct energy scale from the Kondo temperature. This mechanism explains the peculiar magnetic response in $CeIrIn_5$ and the metamagnetic transition in $YbXCu_4$ for $X =$ In as well as the sharp contrast between $X =$ Ag and Cd.

Quantum critical phenomena is one of the most interesting issues in condensed matter physics. Quantum critical points (QCP) emerging when the continuous-transition temperature of symmetry breakings such as magnetic orders is suppressed to absolute zero have been studied intensively [1–3], since the critical fluctuations induce unusual normal-state behaviors and even trigger other instabilities such as unconventional superconductivity [4].

The valence transition is an isostructural phase transition, which is known to occur as a γ-α transition in Ce metal [5] and also in $YbInCu_4$ [6] characterized by a jump of the valence of the Ce and Yb ion. At the critical end point of the first-order valence transition (FOVT), the valence fluctuation diverges as diverging density fluctuations in the liquid-gas transition. When the critical temperature is suppressed by tuning material parameters and enters the Fermi-degeneracy regime, diverging valence fluctuations are considered to be coupled with the Fermi-surface instability. This multiple instability seems to be a key mechanism which dominates the low-temperature properties of the materials including the valence-fluctuating ions such as Ce and Yb [7–10].

Actually, a remarkable increase of the superconducting transition temperature far from antiferromagnetic QCP in $CeCu_2X_2$ ($X =$ Ge, Si) [11–13] and $CeIrIn_5$ [14] as well as linear-temperature dependence of resistivity observed in variety of Ce and Yb compounds [12–17] seems to be a sign of underlying influence of the proximity of the QCP of the valence transition (VQCP) [17].

So far, to reduce the critical temperature of the valence transition toward absolute zero, intensive efforts have been made by chemical substitutions and applying pressure [18]. Usually, magnetic field also offers one of the efficient control parameters. However, it is highly nontrivial how the critical end point as well as the QCP is controlled by applying magnetic field, since valence instabilities are

essentially ascribed to charge degrees of freedom, i.e., relative change of the $4f$- and conduction-electron charges.

In this Letter, we show that magnetic field is an efficient parameter to change the critical end point of the FOVT to the QCP. Unexpectedly, we discover nonmonotonic field dependence of the VQCP in the ground-state phase diagram, whose mechanism is clarified to be cooperative phenomena by Zeeman effect and Kondo effect. We show that a metamagnetic jump in the magnetization is caused by the proximity effect of the VQCP by magnetic field even in the intermediate valence-crossover regime. This mechanism explains a peculiar magnetic response observed in $CeIrIn_5$ [19,20] as well as sharp contrast between $YbAgCu_4$ and $YbCdCu_4$ [15]. Our results indicate the significance of a distinct energy scale, which is characterized by the closeness to the VQCP as a key parameter for the valence-fluctuating materials.

First, we demonstrate how the critical end point is suppressed to absolute zero. Let us consider the Claudius-Clapeyron relation for the FOVT temperature T_v: $\delta T_v/\delta h = -(m_K - m_{MV})/(S_K - S_{MV})$, where m and S denote the magnetization and the entropy, respectively. Here, K represents the Kondo regime where the f-electron (hole) density per site $\langle n_f \rangle$ is close to 1 in the Ce (Yb) system, i.e., $Ce^{3+}4f^1$ and $Yb^{3+}4f^{13}$, and MV represents the mixed-valence regime with $\langle n_f \rangle < 1$ [21]. Since the magnetization as well as the entropy in the Kondo regime are larger than those in the MV regime, as observed in the specific heat and the uniform susceptibility, it turns out that T_v is suppressed by applying h [see Fig. 1(a)]. Then, the critical end point is suppressed to $T = 0$ by h.

Furthermore, the field dependence of T_v in the zero-temperature limit is also derived by using the above relation: For $T \to 0$, the entropy shows the T-linear behavior in both the Kondo and MV regimes and $S_K - S_{MV}$ is approximated to be proportional to T_v in case that T_v is smaller
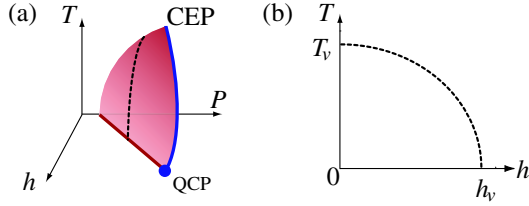
FIG. 1 (color online). (a) Schematic phase diagram, showing the FOVT surface in the T-P-h space, where P represents a control parameter (e.g., pressure, chemical concentration, etc.). The critical end point (CEP) forms a continuous-transition line touched at $T = 0$ as the QCP. (b) FOVT line $(h/h_v)^2 + (T/T_v)^2 = 1$ [22–24] in the T-h plane for a fixed P, corresponding to the dashed line in (a).

than the characteristic energy scales in the Kondo and MV regimes. Noting the temperature independent $m_K - m_{MV}$, we have $\delta T_v/\delta h = -C_1/T_v$, leading to $T_v = C_2\sqrt{h_v - h}$ with constants C_1 and C_2, which explains well the observed behavior in the Ce metal [22] and YbInCu$_4$ [23] [see Fig. 1(b)]. We stress here that our analysis not only provides firm ground for small-T_v behavior by considering the coherence of electrons which is essential for low temperature, but also interpolates high T_v satisfying the relation $(h/h_v)^2 + (T/T_v)^2 = 1$ [22–24] to zero temperature, since this relation was derived by assuming the isolated atomic entropy [22], which is justified only at the high temperature regime.

Although we have shown that the h dependence of the critical end point can be understood from the viewpoint of the free-energy gain by the larger entropy in the Kondo regime, it is highly nontrivial how the VQCP is controlled by h at $T = 0$. To proceed our analysis, we introduce a minimal model which describes the essential part of Ce and Yb systems in the standard notation:

$$H = H_c + H_f + H_{hyb} + H_{U_{fc}} - h\sum_i(S_i^{fz} + S_i^{cz}), \quad (1)$$

where $H_c = \sum_{\mathbf{k}\sigma}\varepsilon_\mathbf{k}c_{\mathbf{k}\sigma}^\dagger c_{\mathbf{k}\sigma}$, $H_f = \varepsilon_f\sum_{i\sigma}n_{i\sigma}^f + U\sum_{i=1}^N n_{i\uparrow}^f n_{i\downarrow}^f$, $H_{hyb} = V\sum_{i\sigma}(f_{i\sigma}^\dagger c_{i\sigma} + c_{i\sigma}^\dagger f_{i\sigma})$, and $H_{U_{fc}} = U_{fc}\sum_{i=1}^N n_i^f n_i^c$. The U_{fc} term is the Coulomb repulsion between the f and conduction electrons, which is considered to play an important role in the valence transition [7,10,25–28]. For example, in the case of Ce metal which exhibits the γ-α transition, the $4f$- and $5d$-electron bands are located at the Fermi level [29]. Since both the orbitals are located on the same Ce site, this term cannot be neglected. In the case of YbInCu$_4$, $H_{U_{fc}}$ also plays a crucial role for the FOVT in the hole picture of Eq. (1) [28].

We apply the slave-boson-mean-field theory [7] to Eq. (1). To describe the state for $U = \infty$, we consider $Vf_{i\sigma}^\dagger b_i c_{i\sigma}$ instead of $Vf_{i\sigma}^\dagger c_{i\sigma}$ in Eq. (1) by introducing the slave-boson operator b_i at the i-th site to describe the f^0 state and require the constraint $\sum_i\lambda_i(\sum_\sigma n_{i\sigma}^f + b_i^\dagger b_i - 1)$ with λ_i being the Lagrange multiplier. For $H_{U_{fc}}$ in Eq. (1),

we employ the mean-field decoupling as $n_i^f n_i^c \simeq n_f n_i^c + n_c n_i^f - \frac{1}{2}n_f n_c$. By approximating mean fields as uniform ones, i.e., $b = \langle b_i\rangle$ and $\bar\lambda = \lambda_i$, the set of mean-field equations is obtained by $\partial\langle H\rangle/\partial\lambda = 0$ and $\partial\langle H\rangle/\partial b = 0$: $\bar\lambda = \frac{V^2}{N}\sum_{\mathbf{k}\sigma}\frac{f(E_{\mathbf{k}\sigma}^-)-f(E_{\mathbf{k}\sigma}^+)}{\sqrt{(\bar\varepsilon_{f\sigma}-\bar\varepsilon_{\mathbf{k}\sigma})^2+4\bar V^2}}$, $1 - |\bar b|^2 = \frac{1}{2N}\sum_{\mathbf{k}\sigma,\pm}[1 \pm \frac{\bar\varepsilon_{f\sigma}-\bar\varepsilon_{\mathbf{k}\sigma}}{\sqrt{(\bar\varepsilon_{f\sigma}-\bar\varepsilon_{\mathbf{k}\sigma})^2+4\bar V^2}}]f(E_{\mathbf{k}\sigma}^\pm)$, and the following equation holds for the total electron number: $\bar n_f + \bar n_c = \sum_{\mathbf{k}\sigma}[f(E_{\mathbf{k}\sigma}^-) + f(E_{\mathbf{k}\sigma}^+)]/N$. Here, $f(E)$ is the Fermi distribution function and $E_{\mathbf{k}\sigma}^\pm$ are the lower ($-$) and upper ($+$) hybridized bands for the quasiparticle with spin σ, respectively: $E_{\mathbf{k}\sigma}^\pm = \frac{1}{2} \times [\bar\varepsilon_{f\sigma} + \bar\varepsilon_{\mathbf{k}\sigma} \pm \sqrt{(\bar\varepsilon_{f\sigma} - \bar\varepsilon_{\mathbf{k}\sigma})^2 + 4\bar V^2}]$, where $\bar\varepsilon_{\mathbf{k}\sigma}$, $\bar\varepsilon_{f\sigma}$ and $\bar V$ are defined by $\bar\varepsilon_{\mathbf{k}\sigma} \equiv \varepsilon_\mathbf{k} + U_{fc}\bar n_f - \frac{h\sigma}{2}$, $\bar\varepsilon_{f\sigma} \equiv \varepsilon_f + \bar\lambda + U_{fc}\bar n_c - \frac{h\sigma}{2}$ and $\bar V \equiv V|\bar b|$. The dispersion of the conduction electrons is taken as $\varepsilon_\mathbf{k} = \mathbf{k}^2/(2m) - D$ with D being the bottom of the conduction band, and the density of states $N_0(\varepsilon)$ is set to satisfy the normalization condition, $\int_{-D}^D d\varepsilon N_0(\varepsilon) = 1$ per spin in three dimension. We take D as the energy unit and show the results for $V = 0.5$ and the total filling $n = (\bar n_f + \bar n_c)/2 = 7/8$.

At $h = 0$ and $T = 0$, a jump in $\bar n_f$ appears as a function of ε_f for large U_{fc}, which indicates the first-order quantum phase transition, since a jump in $\bar n_f$ results in the level crossing of the ground states by the relation $\bar n_f = \partial\langle H\rangle/\partial\varepsilon_f$. The FOVT between the Kondo state and the MV state is caused by U_{fc}, since a large U_{fc} forces the electrons to pour into either the f level or the conduction band. The QCP in the ε_f-U_{fc} plane is identified to be $(\varepsilon_f^{QCP}, U_{fc}^{QCP}) = (0.356, 1.464)$, at which the jump in $\bar n_f$ disappears and the valence susceptibility $\chi_v \equiv -\partial^2\langle H\rangle/\partial\varepsilon_f^2 = -\partial\bar n_f/\partial\varepsilon_f$ diverges. The characteristic energy scale of the system, the so-called Kondo temperature, which is defined as $T_K \equiv \bar\varepsilon_{f\sigma} - \mu$, is estimated to be $T_K = 0.074$ at the QCP.

Note that the surface of the FOVT exists in the parameter space of ε_f, U_{fc}, and V, and a trajectory line is drawn in the space for corresponding experimental parameter such as
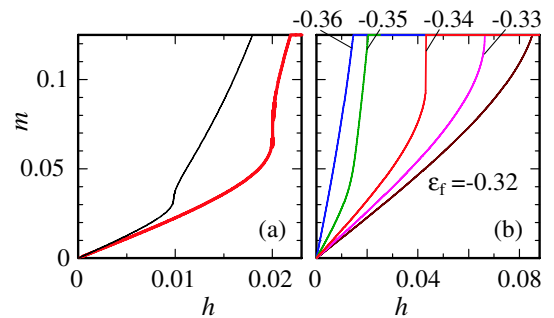

FIG. 2 (color online). m-h curve (a) for $(\varepsilon_f, U_{fc}) = (-0.354, 1.458)$ (thin line) and $(-0.349, 1.442)$ (bold line), and (b) for ε_f ranging from -0.36 to -0.32 at $U_{fc} = 1.42$. In both cases, $D = 1$, $V = 0.5$ at $n = 7/8$.

pressure (i.e., P in Fig. 1). It is also noted that the valence instability is considered to be coupled to the phonon degrees of freedom. Hence, in our model (1), the effect of the hybridization also plays an important role, which might share common aspects with the Kondo-volume-collapse scenario for Ce metal [9].

A remarkable result is found under the magnetic field in the valence-crossover regime for $U_{fc} < U_{fc}^{QCP}$. Figure 2(a) shows the magnetization $m = \sum_i \langle S_i^{fz} + S_i^{cz} \rangle / N$ vs h for $(\varepsilon_f, U_{fc}) = (-0.354, 1.458)$ (thin line) and $(-0.349, 1.442)$ (bold line), indicating that the metamagnetism defined by the diverging magnetic susceptibility $\chi = \partial m / \partial h = \infty$ emerges at $h = h_m = 0.01$ and 0.02, respectively. To clarify the origin, we have determined the FOVT line as well as the QCP under the magnetic field. The result is shown in Fig. 3. It is found that the FOVT line extends to the MV regime, and the location of the QCP is shifted to the smaller U_{fc} and $|\varepsilon_f|$ direction, when h is applied. This low-h behavior of the FOVT line agrees with the low-temperature limit of T_v discussed above.

We show the m-h curve at $U_{fc} = 1.42$ for ε_f ranging from -0.32 to -0.36 in Fig. 2(b). T_K at $h = 0$ is estimated as 0.0353, 0.0873, 0.1346, 0.1611, and 0.1823 for $\varepsilon_f = -0.36, -0.35, -0.34, -0.33,$ and -0.32, respectively (see crosses in Fig. 3). From these results, the mechanism is understood as follows: At $h = 0$, T_K is originally large for $\varepsilon_f = -0.32$ and -0.33, since the system is in the MV regime. However, by applying h, the QCP approaches, which makes T_K reduced, since the system is forced to be closer to the Kondo regime by h. At the magnetic field $h = h_m$ where the QCP is reached, the metamagnetism occurs with a singularity $\delta m \sim \delta h^{1/3}$ [30] as shown in Fig. 2(a). On the other hand, for $\varepsilon_f = -0.35$ and -0.36, the QCP is not approached, so that no metamagnetism appears.

An intriguing result is found in Fig. 3, which exhibits a nonmonotonic h dependence of the QCP: As h increases,
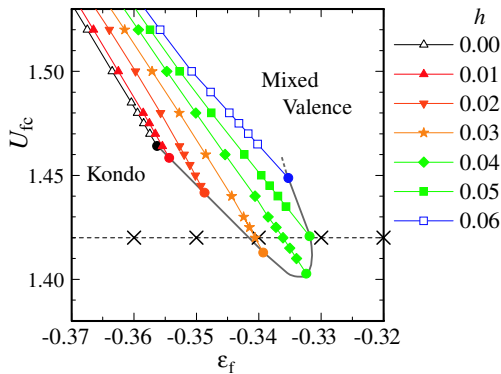

FIG. 3 (color online).   Ground-state phase diagram in the plane of U_{fc} and ε_f for $D = 1$, $V = 0.5$ at $n = 7/8$. The FOVT line with a QCP for $h = 0.00$ (open triangle), 0.01 (filled triangle), 0.02 (inverse triangle), 0.03 (filled star), 0.04 (filled diamond), 0.05 (filled square), and 0.06 (open square). The shaded line connects the QCP under h, which is a guide for the eyes. The dashed line with crosses represents $U_{fc} = 1.42$ (see text).

the QCP shows an upturn around $h = 0.04$, which is comparable to T_K at the QCP for $h = 0$. The upturn of the QCP has been also confirmed for a constant density of states $N_0(\varepsilon) = 1/(2D)$, suggesting that this behavior appears irrespective of details of the band structure.

The nonmonotonic behavior can be understood from the structure of the valence susceptibility χ_v, which is given essentially by the RPA as discussed in Ref. [17]. Namely, it is given as $\chi_v(q) \approx \chi_{fc}^{(0)}(q)/[1 - U_{fc}\chi_{fc}^{(0)}(q)]$, where $\chi_{fc}^{(0)}$ is the bubble diagram composed of f and conduction electrons. In the Kondo regime ($h \lesssim T_K$), where f electrons have a dominant spectral weight at around $\epsilon \sim -\varepsilon_f$ with width $\Delta \simeq \pi V^2 N(\varepsilon_F)$, $\chi_{fc}^{(0)}$ is estimated as $\chi_{fc}^{(0)} \approx 1/|\varepsilon_f|$ and is shown to be an increasing function of h. Therefore, U_{fc}^{QCP} is decreasing as h is applied until it reaches around $h \sim T_K$, and $|\varepsilon_f^{QCP}| \approx U_{fc}^{QCP}$ is also decreasing. For $h \gtrsim T_K$, mass enhancement ($\sim 1/z$) is quickly suppressed, and the MV regime is approached. Then, $\chi_{fc}^{(0)}$ is given as $\chi_{fc}^{(0)} \approx 1/\Delta < 1/|\varepsilon_f|$ with a help of shift of the f level towards the Fermi level, i.e., $\varepsilon_f \to \varepsilon_f + U_{fc}\delta\langle n_c \rangle$ ($\delta\langle n_c \rangle$ being the change of number of conduction electrons per site due to entering the MV regime), so that U_{fc}^{QCP} is larger than that of $U_{fc}^{QCP}(h \sim T_K)$.

We find that h_m corresponds to the difference of T_K at the QCP between $h = 0$ and $h \neq 0$, i.e., $h_m \sim \Delta T_K^{QCP} = T_K^{QCP}(h \neq 0) - T_K^{QCP}(h = 0)$. This indicates emergence of a new energy scale distinct from T_K, which is characterized by the closeness to the VQCP. Furthermore, the proximity of the VQCP to the intermediate valence-crossover regime under h yields emergence of the metamagnetism as well as a jump in m even without showing the temperature-driven FOVT at $h = 0$.

This mechanism explains a peculiar behavior observed in CeIrIn$_5$, which shows a jump in the m-h curve at 42 T, but does not show the first-order transition in any physical quantities when temperature is changed [19,20]. Namely, this is naturally understood if CeIrIn$_5$ is located inside the enclosed area of the QCP line for $h \neq 0$ in Fig. 3. This provides a key to resolve the outstanding puzzle about the origin of the superconductivity of this material, whose transition temperature increases even though antiferromagnetic spin fluctuation is suppressed under pressure [14]. Since superconductivity is shown to appear near the VQCP [7,10], this view verifies a new scenario that the proximity of the VQCP is the origin of the superconductivity.

Our result also explains why the metamagnetic increase appears in the m-h curve in YbAgCu$_4$, but not in YbCdCu$_4$, in spite that both have the comparable T_K's estimated from the $T \to 0$ magnetic susceptibility [15]. The relation $h_m \sim \Delta T_K^{QCP}$ clearly indicates that different h_m can appear for the same T_K according to the location in Fig. 3. Namely, the sharp contrast can be understood if YbAgCu$_4$ and YbCdCu$_4$ are located in the valence-crossover regime for $U_{fc} < U_{fc}^{QCP}$ and ΔT_K^{QCP}, for the
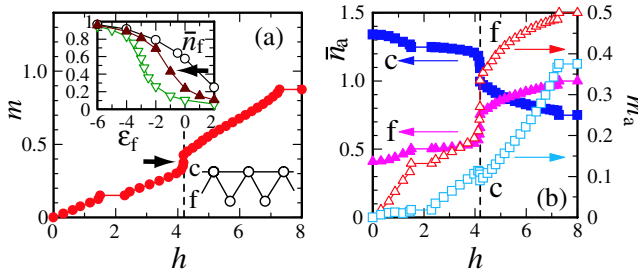
FIG. 4 (color online). Magnetization process for $\varepsilon_k = -2\cos(k)$, $V = 1$, $U = 10^4$, $\varepsilon_f = -1$, and $U_{fc} = 1$ at $n = 7/8$: (a) m-h curve (filled circle). An arrow indicates the metamagnetic transition. Inset: ε_f dependence of $\bar{n}_f$ extrapolated to the bulk limit for $U_{fc} = 0$ (open circle), $U_{fc} = 1$ (filled triangle), and $U_{fc} = 2$ (open triangle). An arrow indicates $\varepsilon_f = -1$. Lattice structure used in the calculation. (b) $\bar{n}_f$ (filled triangle) and $\bar{n}_c$ (filled square). m_f (open triangle) and m_c (open square). In (a) and (b), dashed lines represent $h = h_m$.

former is smaller than that for the latter. Furthermore, the evident FOVT as a function of T [6] as well as a jump in the m-h curve [31] observed in YbInCu$_4$ is also understood if this material is located in the MV regime for $U_{fc} > U_{fc}^{QCP}$ in Fig. 3 [28]. This is consistent with recent band-structure calculations [32].

To examine the mechanism more precisely, we have applied the density-matrix-renormalization-group method to Eq. (1) in one dimension (1D). Since valence fluctuations are basically ascribed to the atomic origin, the fundamental properties are expected to be relevant even in 1D [10]. We show here the results for $\varepsilon_k = -2\cos(k)$, $V = 1$, $U = 10^4$ at $n = 7/8$ on the lattice with $N = 40$ sites for conduction electrons illustrated in the inset of Fig. 4(a), which may be regarded as a 1D mimic of CeIrIn$_5$ and YbXCu$_4$. For $h = 0$, $\bar{n}_f$ vs ε_f for $U_{fc} = 0.0$, 1.0, and 2.0 is shown in the inset of Fig. 4(a). As U_{fc} increases, the change in $\bar{n}_f$ becomes sharp. We show here the magnetization m in the MV state of which $\bar{n}_f$ at $h = 0$ is indicated by an arrow in the inset of Fig. 4(a). A plateau appears at $m = 1 - n = 1/8$, which is expected to disappear if we take more realistic choice of parameters, e.g., the momentum dependence of V and ε_f. The main result is that metamagnetism emerges as indicated by an arrow. The increase of $\bar{n}_f$ simultaneous with the decrease of $\bar{n}_c$ at $h = h_m$ shown in Fig. 4(b) reveals that this is caused by the field-induced extension of the QCP to the MV regime. Namely, these results indicate that the mean-field conclusion is not altered even after taking account of quantum fluctuations and electron correlations.

To explore further the nature of this metamagnetism, we have calculated $m_f = \sum_i \langle S_i^{fz} \rangle / N$ and $m_c = \sum_i \langle S_i^{cz} \rangle / N$, and we find that m_c decreases at $h = h_m$, while m_f increases as shown in Fig. 4(b). Since the Kondo cloud is still formed even at $h = h_m$, i.e., $\langle \mathbf{S}_i^f \cdot \mathbf{S}_i^c \rangle < 0$, a remarkable decrease of $\langle S_i^{cz} \rangle$ is ascribed to the field-induced Kondo

effect, which is a consequence of the energy benefit by both the Kondo effect and the Zeeman effect. Although this mechanism itself has been known to occur in the Kondo regime [33], the present finding is that such a mechanism works in the MV regime as a driving force of the field-induced VQCP.

In summary, we have clarified the novel mechanism of the magnetic-field dependence of critical points of valence transitions, and we believe that the proximity of the VQCP revealed in this study provides an essential ingredient to understand the T-P-h phase diagram of the Ce and Yb systems.

[1] T. Moriya, *Spin Fluctuations in Itinerant Electron Magnetism* (Springer-Verlag, Berlin, 1985).
[2] J. A. Hertz, Phys. Rev. B **14**, 1165 (1976).
[3] A. J. Millis, Phys. Rev. B **48**, 7183 (1993).
[4] G. R. Stewart, Rev. Mod. Phys. **73**, 797 (2001).
[5] K. A. Gschneidner and L. Eyring, *Handbook on the Physics and Chemistry of Rare Earths* (North-Holland, Amsterdam, 1978).
[6] I. Felner and I. Nowik, Phys. Rev. B **33**, 617 (1986).
[7] Y. Onishi *et al.*, J. Phys. Soc. Jpn. **69**, 3955 (2000).
[8] P. Monthoux *et al.*, Phys. Rev. B **69**, 064517 (2004).
[9] M. Dzero *et al.*, Phys. Rev. Lett. **97**, 185701 (2006).
[10] S. Watanabe *et al.*, J. Phys. Soc. Jpn. **75**, 043710 (2006).
[11] D. Jaccard *et al.*, Physica B (Amsterdam) **259–261**, 1 (1999).
[12] A. T. Holmes *et al.*, Phys. Rev. B **69**, 024508 (2004).
[13] H. Q. Yuan *et al.*, Science **302**, 2104 (2003).
[14] S. Kawasaki *et al.*, Phys. Rev. Lett. **94**, 037007 (2005).
[15] J. L. Sarrao *et al.*, Phys. Rev. B **59**, 6855 (1999).
[16] S. Wada and A. Yamamoto (private communications).
[17] K. Miyake, J. Phys. Condens. Matter **19**, 125201 (2007).
[18] J. M. Lawrence *et al.*, Phys. Rev. B **29**, 4017 (1984).
[19] T. Takeuchi *et al.*, J. Phys. Soc. Jpn. **70**, 877 (2001).
[20] E. C. Parm *et al.*, Physica B (Amsterdam) **329–333**, 587 (2003).
[21] We refer to spatially uniform and quantum mechanically valence-fluctuating state with $\langle n_f \rangle < 1$ as mixed valence. We refer to the state with larger $\langle n_f \rangle$ than that in the mixed-valence state at the first-order transition as the Kondo state. Note that in the intermediate-coupling regime, $\langle n_f \rangle$ in the Kondo state is smaller than 1.
[22] F. Drymiotis *et al.*, J. Phys. Condens. Matter **17**, L77 (2005).
[23] C. D. Immer *et al.*, Phys. Rev. B **56**, 71 (1997).
[24] S. Basu *et al.*, Physica B (Amsterdam) **378–380**, 686 (2006).
[25] C. E. T. Goncalves da Silva *et al.*, Solid State Commun. **17**, 1521 (1975).
[26] A. C. Hewson *et al.*, Solid State Commun. **22**, 379 (1977).
[27] I. Singh *et al.*, Solid State Commun. **34**, 65 (1980).
[28] J. K. Freericks *et al.*, Phys. Rev. B **58**, 322 (1998).
[29] W. E. Pickett *et al.*, Phys. Rev. B **23**, 1266 (1981).
[30] A. J. Millis *et al.*, Phys. Rev. Lett. **88**, 217204 (2002).
[31] K. Yoshimura *et al.*, Phys. Rev. Lett. **60**, 851 (1988).
[32] H. Harima (unpublished).
[33] S. Watanabe, J. Phys. Soc. Jpn. **69**, 2947 (2000).